

Extraction of Temporal Gait Parameters using a Reduced Number of Wearable Accelerometers

Mohamed Boutaayamou^{1,2}, Vincent Denoël¹, Olivier Brûls¹, Marie Demonceau³, Didier Maquet³,
Bénédicte Forthomme¹, Jean-Louis Croisier¹, Cédric Schwartz¹, Jacques G. Verly²
and Gaëtan Garraux^{4,5}

¹Laboratory of Human Motion Analysis, University of Liège (ULg), Liège, Belgium

²INTELSIG Laboratory, Department of Electrical Engineering and Computer Science, ULg, Liège, Belgium

³Department of Rehabilitation and Movement Sciences, ULg, Liège, Belgium

⁴Movere Group, Cyclotron Research Center, ULg, Liège, Belgium

⁵Department of Neurology, University Hospital Center, Liège, Belgium

Keywords: Gait Analysis, Wearable Accelerometers, Wavelet Analysis, Validation, Gait Segmentation, Gait Events, Heel-off, Heel Strike, Toe Strike, Toe-off, Heel Clearance, Stance Time, Swing Time, Stride Time.

Abstract: Wearable inertial systems often require many sensing units in order to reach an accurate extraction of temporal gait parameters. Reconciling easy and fast handling in daily clinical use and accurate extraction of a substantial number of relevant gait parameters is a challenge. This paper describes the implementation of a new accelerometer-based method that accurately and precisely detects gait events/parameters from acceleration signals measured from only two accelerometers attached on the heels of the subject's usual shoes. The first step of the proposed method uses a gait segmentation based on the continuous wavelet transform (CWT) that provides only a rough estimation of motionless periods defining relevant local acceleration signals. The second step uses the CWT and a novel piecewise-linear fitting technique to accurately extract, from these local acceleration signals, gait events, each labelled as heel strike (HS), toe strike (TS), heel-off (HO), toe-off (TO), or heel clearance (HC). A stride-by-stride validation of these extracted gait events was carried out by comparing the results with reference data provided by a kinematic 3D analysis system (used as gold standard) and a video camera. The temporal accuracy \pm precision of the gait events were for HS: $7.2 \text{ ms} \pm 22.1 \text{ ms}$, TS: $0.7 \text{ ms} \pm 19.0 \text{ ms}$, HO: $-3.4 \text{ ms} \pm 27.4 \text{ ms}$, TO: $2.2 \text{ ms} \pm 15.7 \text{ ms}$, and HC: $3.2 \text{ ms} \pm 17.9 \text{ ms}$. In addition, the occurrence times of right/left stance, swing, and stride phases were estimated with a mean error of $-6 \text{ ms} \pm 15 \text{ ms}$, $-5 \text{ ms} \pm 17 \text{ ms}$, and $-6 \text{ ms} \pm 17 \text{ ms}$, respectively. The accuracy and precision achieved by the extraction algorithm for healthy subjects, the simplification of the hardware (through the reduction of the number of accelerometer units required), and the validation results obtained, convince us that the proposed accelerometer-based system could be extended for assessing pathological gait (e.g., for patients with Parkinson's disease).

1 INTRODUCTION

Wearable inertial systems have been proposed to measure gait events and to estimate temporal gait parameters (e.g., Willemsen et al. 1990; Aminian et al., 1999; Selles et al., 2005; Lee et al. 2007; Godfrey et al., 2008). Compared to conventional gait analysis techniques, such as optoelectronic motion capture systems and instrumented walkways, these systems are not limited to controlled laboratory environment; they can handle gait analysis in an entirely natural setting with the possibility to obtain

gait parameters over longer walking distances (e.g., Khandelwal and Wickström 2014). The hardware part of inertial systems, such as accelerometer units, includes low-cost, small, and lightweight sensing units with generally low power consumption (e.g., Stamatakis et al., 2011). With an appropriate algorithm, these inertial systems are particularly suitable for assessing gait in a clinical environment (e.g., Salarian et al., 2004; Rueterbories et al., 2010).

Yet, these systems often need many sensing units to achieve reasonable accuracy and precision in the extraction of gait events/parameters. Arranging these

sensor units on lower limbs (e.g., feet) in a manner that is acceptable for clinical gait analysis remains a challenge.

We have previously developed and validated a signal processing algorithm to automatically extract gait events in healthy walking – labelled as heel strike (HS), toe strike (TS), heel-off (HO), and toe-off (TO) – from acceleration signals measured by four accelerometer units attached to heels and toes (Boutaayamou et al., 2015a). The algorithm exploited distinctive and remarkable features in these acceleration signals to identify and extract gait events with good accuracy and precision.

In this paper, we present a new signal processing algorithm that extracts the same gait events from only two accelerometers, i.e., one on each shoe, at the level of the heel. Our approach to the aforementioned problem consists therefore in reducing the number of accelerometer units by eliminating the two units on the toes. We also extend the previous algorithm to detect a new gait event, i.e., the time of heel clearance (HC) which is an important gait event that can refine the swing phase. In addition, we consider the validation on a stride-by-stride basis of the proposed algorithm on a group of healthy people during normal walking. In this validation, we compare the results (i.e., measured gait events and calculated temporal gait parameters of interest) to reference data provided by a kinematic 3D system (used as gold standard) and a video camera.

2 METHOD

2.1 Wearable Accelerometer System

Acceleration signals during walking were recorded by a wearable, wireless accelerometer-based hardware system which includes several small three-axis accelerometer units (2 cm x 1 cm x 0.5 cm), a transmitter module, and a receiver module (Stamatakis et al., 2011; Boutaayamou et al., 2015a) (Figure 1). This system can measure accelerations up to ± 12 g (where $g = 9.81$ m/s² is value of the gravitational acceleration) along its three sensitive axes: x (horizontal), y (transverse), and z (vertical). In this study, two accelerometer units were tightly attached on the right and left feet, i.e., one on each shoe at the level of the heel. The right and left accelerometers were synchronized. Accelerometers were connected to the transmitter module positioned on the waist. The wires between accelerometers and

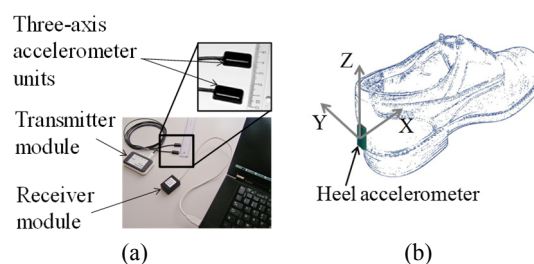


Figure 1: (a) The wearable accelerometer-based hardware system. (b) Schematic illustration of the placement of a wearable accelerometer (either for right or left foot) and the direction of axes.

the transmitter module were tightly strapped around the legs so as to avoid disturbing the subject movements. Acceleration signals were recorded at 200 Hz. All data were analyzed using Matlab 7.6.0 (MathWorks, Natick, MA, USA).

2.2 Subjects and Gait Tests Procedure

Gait signals were recorded during walking tests performed by seven young and healthy subjects without any previous injury of the lower limbs ((mean \pm standard deviation) age = 27 ± 2.6 years; height = 181 ± 7 cm; weight = 78 ± 9 kg). All of them provided informed consent. The gait tests procedure of this study is similar to the one reported in (Boutaayamou et al., 2015a). Before we started the measurements, subjects took sufficient time to get used to the instrumentation tools and the experimental procedure. During the tests, they were asked to walk on a 12-m long track, at their preferred, self-selected, usual speed. Each subject performed several gait tests of 60 s. Subjects wore their own regular shoes. All of the walking tests were performed at the Laboratory of Human Motion Analysis of the University of Liège, Belgium.

2.3 Wavelet Analysis: Segmentation of Acceleration Signals

In the present study, we use a segmentation method that we have previously developed (Boutaayamou et al., 2015b) to identify gait patterns from only heel acceleration signals, thereby reducing the number of wearable accelerometers and allowing for a robust extraction of the gait events/parameters (see Sec. 2.4). This segmentation method is based on the continuous wavelet transform (CWT) to isolate (1) time intervals where the heel acceleration is close to zero, from (2) time intervals the accelerometers are moving. The wavelet coefficient $C(a,b)$ of the CWT

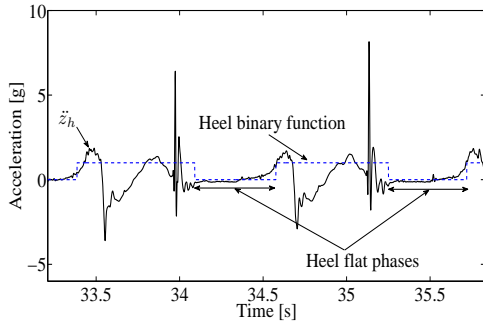


Figure 2: Rough estimation of heel flat/non-flat phases using the gait segmentation based on the continuous wavelet transform.

of a signal $s(t)$ is defined as

$$C(a, b) = \frac{1}{\sqrt{|a|}} \int_{-\infty}^{+\infty} s(t) \psi^* \left(\frac{t-b}{a} \right) dt, \quad (1)$$

where a ($\neq 0$) and b ($\in \mathbb{R}$) are the scale and location parameters, respectively, ψ^* is the complex conjugate of the mother wavelet function ψ , and t is the time. Compressing a (small values of a) tracks high frequencies changes whereas stretching a (large values of a) tracks low frequencies. $C(a, b)$ thus measures the similarity between the signal $s(t)$ and the scaled and shifted versions of ψ , with larger values indicating higher similarity. The wavelet (Mexican hat) is chosen here as the mother wavelet ψ .

The detailed description of the developed segmentation method is not the focus of this study. Rather, we consider the results of its application to the vertical acceleration signal measured at the level of the heel. We therefore obtain a “heel binary function” that roughly estimate heel flat phases (motionless periods) and heel non-flat phases. A typical result of the binary function is shown in Figure 2 (dashed lines). The segmentation method has the advantage that it avoids to look directly for specific gait events. The segmentation only determine rough heel flat/non-flat phases in which gait events of interest can be further extracted with good accuracy.

2.4 New Signal Processing Algorithm

In order to estimate precisely gait parameters such as the durations of the stance, swing, and stride phases during a gait cycle (i.e., the duration of a stride), it is necessary to detect, for each foot, the precise moments of gait events of interest during the same gait cycle. These gait events are characterized by distinctive and remarkable features on heel

acceleration signals. Depending on the nature of these features, a suitable method is employed in the present study to accurately extract gait events. For clarity, we consider only one foot. It is obvious that the algorithm could be applied in the same way for both feet.

Times of occurrence of HS_{accel} , TS_{accel} , HO_{accel} , TO_{accel} , and HC_{accel} are identified mainly from the acceleration signals in sagittal plane, i.e., with respect to the x -axis and z -axis accelerations denoted by \ddot{z}_h and \ddot{x}_h , respectively. The subscripts $accel$, ref , and h refer to our method, to the reference methods, and to the heel, respectively.

2.4.1 Gait Events Identification

We now describe the main steps of the detection following the chronological occurrence order of healthy gait events (i.e., not the order that the algorithm follows to extract these events).

a) The time of the heel strike event: HS_{accel}

In the present study, we adapt the method described in (Boutaayamou et al., 2015a) to detect HS_{accel} as follows:

- At HS_{accel} , the heel acceleration signal \ddot{z}_h is subject to abrupt changes (Figure 3a). To detect HS_{accel} , we only consider the segment defined as the second half of the heel non-flat phase. In this segment, HS_{accel} is identified using the magnitude of \ddot{z}_h filtered with a 4th-order zero-lag Butterworth high-pass filter (cutoff frequency=10 Hz). HS_{accel} is detected as the time of occurrence of the maximum value of the magnitude of this filtered \ddot{z}_h (Figure 3a). As pointed out in (Boutaayamou et al., 2015a), the determination of HS_{accel} is robust with respect to this filtering step, since HS_{accel} occurs rapidly with a frequency larger than 10 Hz.

b) The time of the toe strike event: TS_{accel}

TS_{accel} can be extracted from the heel acceleration signal as the accelerometer is sensitive enough to measure the acceleration movement of the foot when the toe hits the ground. The main steps to estimate TS_{accel} are as follows:

- As TS_{accel} occurs after HS_{accel} and before HO_{accel} , we seek TS_{accel} in the segment $[HS_{accel}, 0.4*HS_{accel} + 0.6*HO_{accel}]$ (the procedure for extracting HO_{accel} is explained in c)). TS_{accel} is automatically detected using \ddot{x}_h and \ddot{z}_h restricted to this segment. The resulting local signals are then filtered with a 4th-order zero-lag Butterworth low-pass filter (cutoff frequency = 20 Hz), and integrated twice in order to calculate their associated position signals. The

drift related to this double integration is limited since the latter is performed in a small time interval. We then apply a piecewise-linear fitting method to each of these position signals. This method estimates a location of convex curvature in a signal using two linear segment that best fit this signal in the least-square sense (Appendix) (Boutaayamou et al., 2015a). The times of resulting convex curvatures in the two position signals are denoted t_1 and t_2 . It is then assumed that TS_{accel} is estimated as the mean of t_1 and t_2 (Figure 3b).

c) The time of the heel-off event: HO_{accel}

HO_{accel} is automatically detected in the segment that lies between 125 ms after HS_{accel} and 70 ms before TO_{accel} (the extraction method of TO_{accel} is described in d)). We adapt the method presented in (Boutaayamou et al., 2015a) to detect HO_{accel} from \ddot{z}_h as follows:

- We consider the local signal obtained from the restriction of \ddot{z}_h to the previous segment. This local signal is then filtered with a 4th-order zero-lag Butterworth low-pass filter (cutoff frequency = 20 Hz). This filtering step does not alter the physical significance of the local signal (Boutaayamou et al., 2015a). Since this signal corresponds to a slow movement (some milliseconds before and after HO_{accel}), there is no critical peak to be detected that could be removed erroneously in this filtering step (Boutaayamou et al., 2015a). A double integration of this local acceleration signal is then performed to calculate the corresponding position signal. The drift that could be generated from this double integration is negligible since the latter is carried out in a small time interval. We apply the aforementioned piecewise-linear fitting method twice to the resulting local position signal in order to estimate successive locations of convex curvature in this local position signal. The time of the last location of convex curvature is our estimate of HO_{accel} (Figure 3c).

d) The time of the toe-off event: TO_{accel}

- At TO_{accel} , the direction of motion of the ankle joint changes from plantarflexion to dorsiflexion in the sagittal plane (Whittle, 1996). It is assumed that TO_{accel} corresponds to the time when a zero crossing of the vertical heel acceleration signal occurs after the beginning of the non-flat phase (Figure 3d).

e) The time of the heel clearance event: HC_{accel}

- HC_{accel} is defined as the moment when the minimum clearance between the heel accelerometer and the ground is achieved during the swing phase. We consider distinctive vertical heel acceleration features that indicate where HC_{accel} can be found in the time and frequency domains. These features are rather sharp negative peaks in \ddot{z}_h (Figure 3e) involving some mid frequencies. In order to extract HC_{accel} , we apply the CWT (see Sec. 2.3) to the local signal defined as the restriction of \ddot{z}_h to the neighbourhood of these features. The CWT is indeed adapted for identifying HC_{accel} because it allows detection of a specified frequency at a specified time. The previous local signal is then decomposed into wavelet packages. The wavelet (Mexican hat) is used as the mother wavelet to extract HC_{accel} as it is similar to the pattern of the aforementioned features. A typical result is depicted in Figure 3e.

2.4.2 Extraction of Temporal Gait Parameters

Temporal gait parameters, such as durations of the stance, swing, and stride phases, are calculated on the basis of the previous gait events as follows:

- Right stance duration (time between right HS (HS_{right}) and right TO (TO_{right}) during stride i)

$$Right\ stance = TO_{right}(i) - HS_{right}(i).$$

- Left stance duration (time between left HS (HS_{left}) and left TO (TO_{left}) during stride i)

$$Left\ stance = TO_{left}(i) - HS_{left}(i).$$

- Right swing duration (time between HS_{right} of stride $i+1$ and TO_{right} of stride i)

$$Right\ swing = HS_{right}(i+1) - TO_{right}(i).$$

- Left swing duration (time between HS_{left} of stride $i+1$ and TO_{left} of stride i)

$$Left\ swing = HS_{left}(i+1) - TO_{left}(i).$$

- Right stride duration (time between two consecutive right HSs)

$$Right\ stride = HS_{right}(i+1) - HS_{right}(i).$$

- Left stride duration (time between two consecutive left HSs)

$$Left\ stride = HS_{left}(i+1) - HS_{left}(i).$$

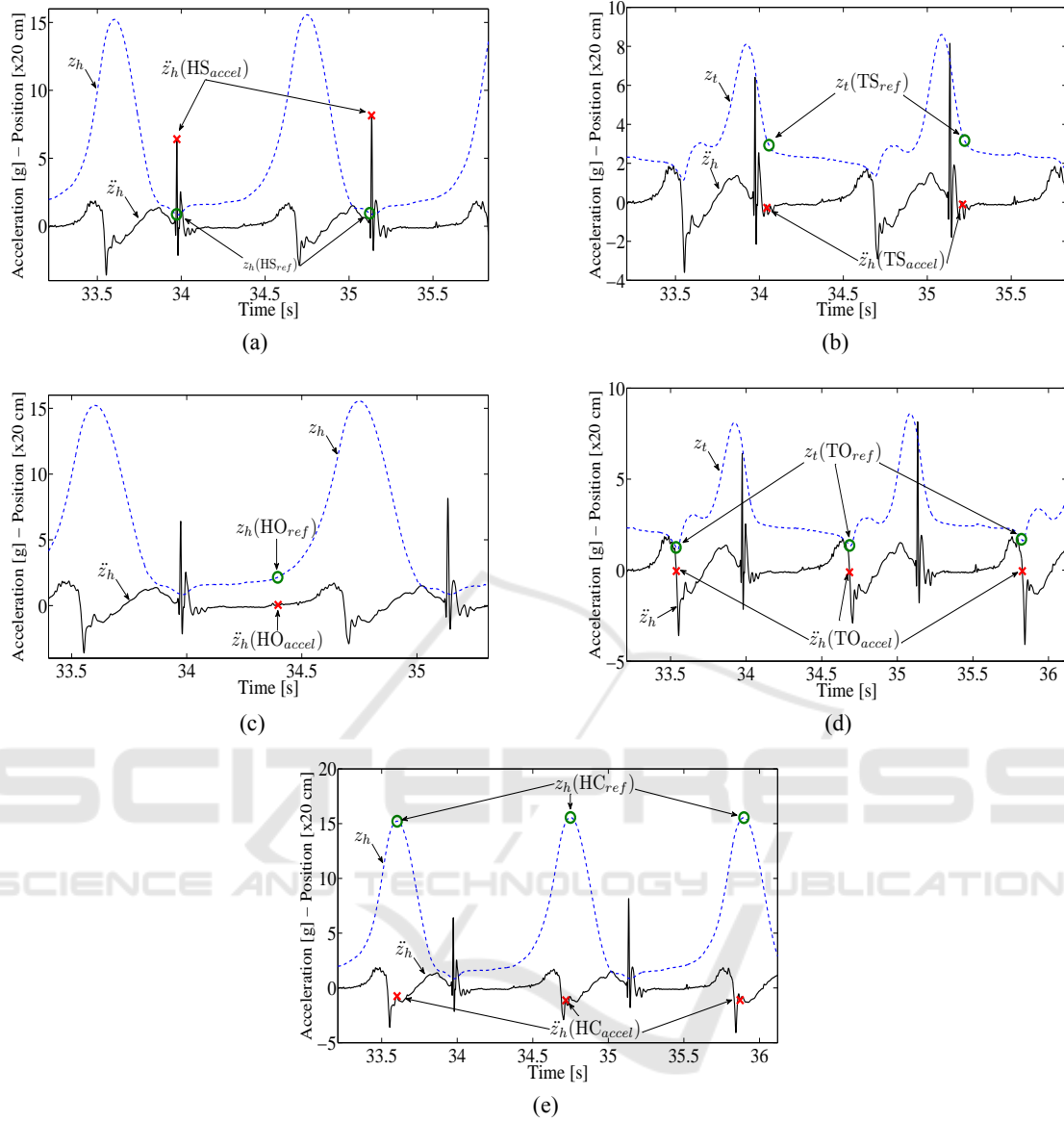


Figure 3: Vertical heel acceleration signal (i.e., \ddot{z}_h measured by our accelerometer system) and reference kinematic signals (i.e., the vertical heel position z_h and the vertical toe position z_t measured by the Codamotion system). The gait events, i.e., (a) HS, (b) TS, (c) HO, (d) TO, and (e) HC, detected by our method and by reference methods are shown on each signal during typical consecutive strides.

2.5 Stride-by-stride Validation Method

2.5.1 Reference Data

A kinematic 3D analysis system (Codamotion system; Charnwood Dynamics; Rothley, UK) and a video camera provided reference data to validate, on a stride-by-stride basis, the gait parameters/events determined by our method.

The kinematic system is based on active optical

technology; it can accurately measure the 3D positions of active markers placed in the body locations of interest. We collected kinematic data at the level of the heel and the toe of each foot at 400 Hz. The heel marker was placed upon the heel accelerometer. The video camera (30 fps) was placed close to the track such that the pointing direction is approximately perpendicular to the sagittal plan.

Kinematic data were used to validate, on a stride-by-stride basis, the gait events HS_{accel} , TS_{accel} ,

Table 1: The results of our method are compared to the results of reference methods considering several consecutive strides. This evaluation is given as the accuracy (mean of the differences), the precision (std. dev. of the differences), limits of agreement, 95% confidence interval (CI) of the differences, and 95% CI of the lower and upper limits of agreement.

	Accuracy (ms) (precision (ms))	Limits of agreements (ms)	95% CI of the differences (ms)	95% CI of the lower limits (ms)	95% CI of the upper limits (ms)	No. of events
HS	7.2 (22.1)	[-36.2 50.7]	[5.6 8.8]	[-38.9 - 33.5]	[47.9 53.4]	771
TS	0.7(19.0)	[-36.6 38.0]	[-0.9 2.3]	[-39.3 - 33.9]	[35.3 40.7]	567
HO	-3.4 (27.4)	[-57.2 50.3]	[-8.2 1.3]	[-66.5 - 49.9]	[43.1 59.7]	126
TO	2.2 (15.7)	[-28.6 33.0]	[1.1 3.3]	[-30.5 - 26.8]	[31.2 34.9]	819
HC	3.2 (17.9)	[-31.9 38.3]	[1.9 4.4]	[-34.7 - 30.5]	[36.9 41.1]	839

TO_{accel} , and HC_{accel} . Reference gait events HS_{ref} and TO_{ref} , were obtained by the kinematic method reported in (Boutaayamou et al., 2014). HS_{ref} and TO_{ref} were extracted solely from measured heel and toe coordinates during overground walking (Figures 3a and 3d). TS_{ref} was extracted from the vertical toe position signal (Boutaayamou et al., 2015a) in each gait cycle (Figure 3b). HC_{ref} was detected as the time of the local maximum of heel clearance (Figure 3e). The video camera provided HO_{ref} .

2.5.2 Evaluation Method

We evaluated the level of agreement between our method and the reference methods by quantifying the accuracy, precision, absolute error, and intraclass correlation coefficient (ICC). Accuracy and precision were computed as the mean and standard deviation (std. dev.), respectively, of the differences between the gait events for each stride, i.e., $HS_{accel} - HS_{ref}$, $TS_{accel} - TS_{ref}$, $HO_{accel} - HO_{ref}$, $TO_{accel} - TO_{ref}$, and $HC_{accel} - HC_{ref}$. The absolute error was calculated as the mean and std. dev. of absolute values of the previous differences. The ICC evaluates the statistical agreement between our method and the reference methods. A Bland-Altman analysis was also carried out.

3 RESULTS

Table 1 provides a quantitative one-by-one comparison of gait events. Because of the limited number of extracted reference events and the variation of some reference patterns among subjects, the sample size for the compared gait events was not always the same but ranged between 126 and 839 events. During some gait tests, we observed that some markers – used to record reference kinematic signals – detached from the shoes. We therefore excluded the associated gait events from the

analysis. In addition, we emphasize that HO_{ref} was obtained only by the video camera. The extraction of HO_{ref} is thus limited to one stride during a given gait test. The total number of HO_{ref} (here 126) is therefore much smaller than that of HS_{ref} , TS_{ref} , TO_{ref} , and HC_{ref} . The four latter reference data were indeed extracted from consecutive strides.

The accuracy and precision of gait events detection ranged from -3.4 ms to 7.2 ms, and 15.7 ms to 27.4 ms, respectively. Given the sampling frequency of 200 Hz of the recorded heel accelerations for both feet, the accuracy and the precision of detection are less than durations of 2 frames (10 ms) and 6 frames (30 ms), respectively.

Figure 4 shows the Bland-Altman plots of gait events differences. We observe small systematic biases in accordance with the accuracy of detection provided in Table 1. The proposed method tends to detect earlier gait events except for HO. In addition, the limits of agreement (i.e., mean \pm 1.96 std. dev.) and their associated 95% confidence interval exhibit small variations in the times of gait events (Table 1).

Table 2 shows the results of durations of stance, swing, and stride phases calculated by our method and by the reference method (i.e., provided by the Codamotion system) for the right and left feet. These temporal parameters could be estimated with a mean absolute error less than 15 ms. The ICC coefficient was larger than 0.95 for both stance time and stride time, and larger than 0.87 for swing time.

Figure 5 shows the Bland-Altman plots of the temporal parameters for the right and left feet. Most differences of these temporal parameters are within the 1.96 std. dev. lines.

4 DISCUSSION

We have presented a new signal processing algorithm that extracts relevant temporal gait

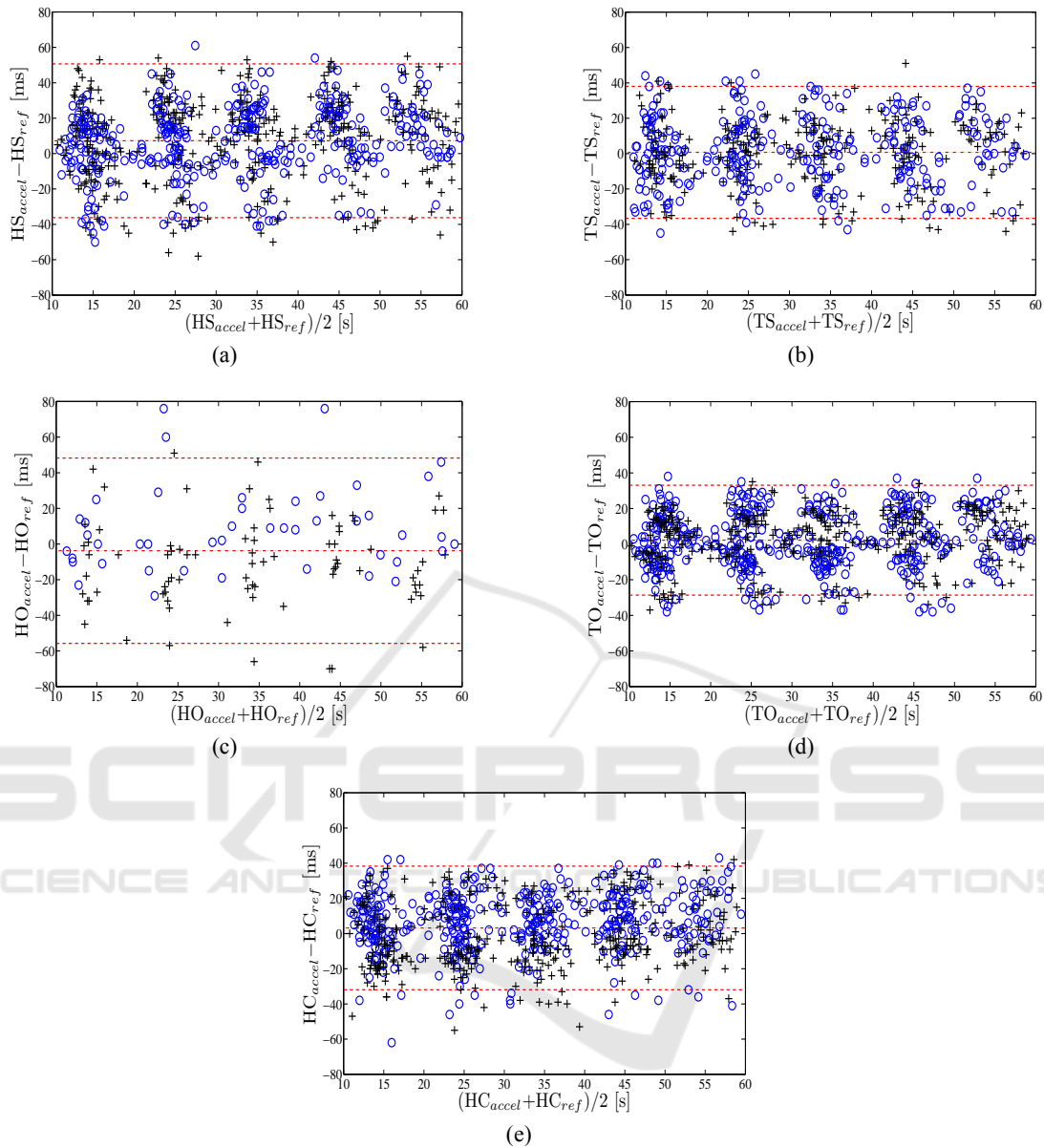


Figure 4: Bland–Altman plots of the gait events, i.e., (a) HS, (b) TS, (c) HO, (d) TO, and (e) HC, measured using our method and reference methods, with mean (dash-dotted line in the middle) of differences $HS_{accel} - HS_{ref}$, $TS_{accel} - TS_{ref}$, $HO_{accel} - HO_{ref}$, $TO_{accel} - TO_{ref}$, and $HC_{accel} - HC_{ref}$. 95% of these differences are between the lines ± 1.96 std. dev. (dashed lines). (○) and (+) refer to gait events measured at the right foot and those measured at the left foot, respectively.

parameters/events from only two accelerometers attached to the right and left feet, i.e., one on each shoe at the level of the heel.

The new algorithm is versatile enough to detect gait events. The algorithm is based on the CWT and an original piecewise-linear fitting method. Those methods allow for an automatic and robust extraction of gait events from relevant local acceleration signals. The algorithm was validated by

comparing results obtained by our method to those obtained by a kinematic 3D system (used as gold standard) and a video camera. The experimental results show a good agreement between our algorithm and the reference, and demonstrate an accurate and precise detection of HS, TS, HO, TO, and HC in a group of healthy people during normal walking. In addition, the algorithm computes the time of stance, swing, and stride phases with a good

Table 2: Results of right/left stance, swing, and stride phase durations calculated by our method are compared to those obtained by a reference kinematic system, Codamotion, used as gold standard. This comparison is given as the difference of the estimated values (mean error), the mean of the absolute error (abs. error), and the intraclass correlation coefficient (ICC).

Gait parameters	Foot	Accelerometers	Codamotion	Mean error	Abs. error	ICC	No. of strides
Stance time (s)	Right	0.670 ± 0.047	0.674 ± 0.055	-0.004 ± 0.016	0.012 ± 0.011	0.95	188
	Left	0.656 ± 0.052	0.662 ± 0.055	-0.006 ± 0.015	0.012 ± 0.010	0.95	220
	Right and left	0.662 ± 0.050	0.668 ± 0.055	-0.006 ± 0.015	0.012 ± 0.010	0.95	408
Swing time (s)	Right	0.404 ± 0.042	0.399 ± 0.035	0.005 ± 0.018	0.014 ± 0.012	0.89	336
	Left	0.418 ± 0.038	0.413 ± 0.035	0.005 ± 0.018	0.014 ± 0.011	0.87	383
	Right and left	0.412 ± 0.041	0.407 ± 0.035	-0.005 ± 0.017	0.014 ± 0.011	0.88	719
Stride time (s)	Right	1.080 ± 0.092	1.083 ± 0.092	-0.003 ± 0.016	0.012 ± 0.011	0.98	181
	Left	1.081 ± 0.090	1.089 ± 0.098	-0.008 ± 0.018	0.015 ± 0.013	0.98	227
	Right and left	1.080 ± 0.090	1.087 ± 0.095	-0.006 ± 0.017	0.013 ± 0.012	0.98	408

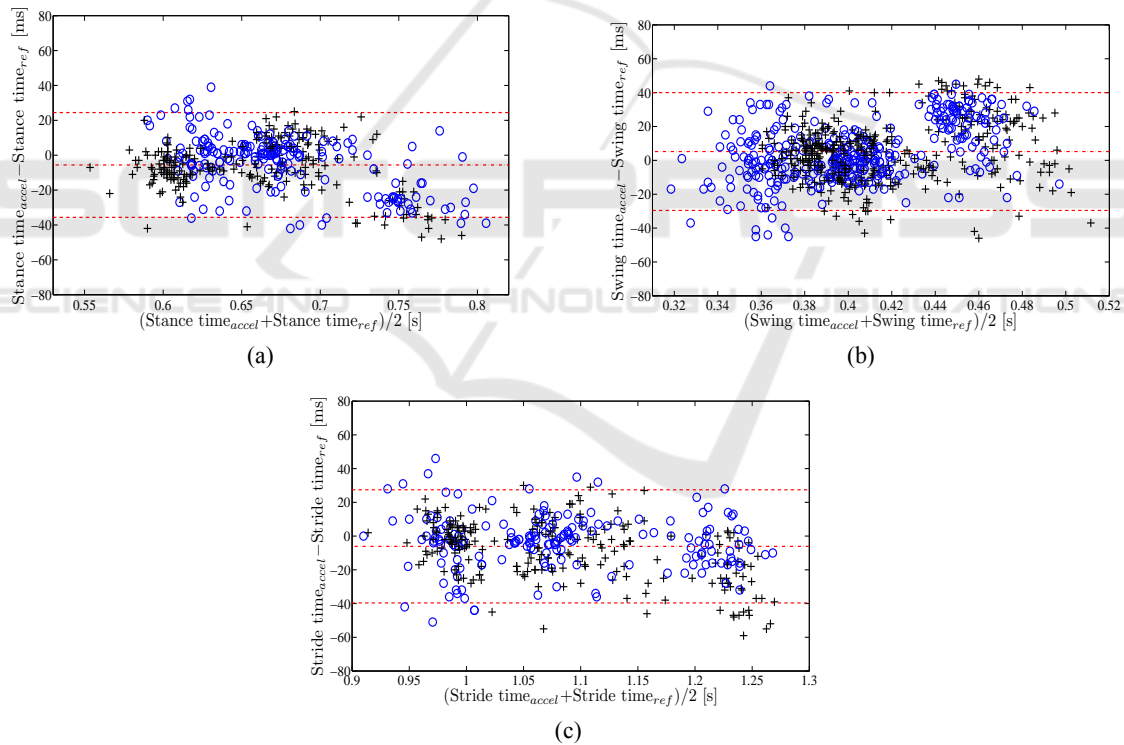


Figure 5: Bland–Altman plots of the temporal gait parameters, i.e., (a) stance time, (b) swing time, and (c) stride time estimated during consecutive strides by our method and the gold standard method. (o) and (+) refer to right and left gait parameters, respectively.

accuracy and precision.

Previous studies reported results of gait parameters during the normal walk. Compared to stance time calculated in (Selles et al., 2005) (i.e., $15 \text{ ms} \pm 41 \text{ ms}$), in (Rampp et al., 2015) (i.e.,

$9 \text{ ms} \pm 69 \text{ ms}$), and in (Salarian et al., 2004) (i.e., $5.9 \text{ ms} \pm 29.6 \text{ ms}$), the accuracy is similar but the precision is improved in our method (i.e., $-6 \text{ ms} \pm 15 \text{ ms}$). Similar accuracy and better precision in stride time are also found in our method

(i.e., $-6 \text{ ms} \pm 17 \text{ ms}$) compared to (Rampp et al., 2015) (i.e., $2 \text{ ms} \pm 68 \text{ ms}$) and to (Salarian et al., 2004) (i.e., $2.2 \text{ ms} \pm 23.2 \text{ ms}$). In addition, the accuracy of swing time in (Rampp et al., 2015) (i.e., $-8 \text{ ms} \pm 45 \text{ ms}$) is similar to our results but the precision is improved in our method (i.e., $-5 \text{ ms} \pm 17 \text{ ms}$). Compared to commercial trunk accelerometer systems (e.g., (Auvinet et al., 1999)), which only provide global gait features, our system is capable to extract stride-by-stride parameters. The stride-by-stride extraction may be a huge advantage in the gait analysis of some specific population such as Parkinson's disease patients who experience freezing of gait, a sudden and brief episodic alteration of strides regulation.

Participants did not complain about the hardware system during the gait tests. They all reported that wires and accelerometers did not interfere with their gait. Since only two accelerometers were attached to heels and wires were behind the legs of the participants during walking, these participants did not notice or complain about the system.

It is noteworthy that all accelerometers of the used hardware system were synchronized. The algorithm can thus extract other important gait parameters such as the times of initial double support, terminal double support, double support, and right/left steps.

Based on TS and HO, the algorithm can extract the durations of the sub-phases of the stance phase, namely: (1) loading response duration (time from HS of one foot to TS of the same foot); (2) foot-flat duration (time from TS of one foot to HO of the same foot); and (3) push-off duration (time from HO of one foot to TO of the same foot). In addition, HC can be used to refine the swing phase duration.

The proposed ambulatory accelerometer system was capable of measuring temporal gait parameters in a very large number of strides without the need of controlled laboratory conditions. We believe that our novel accelerometer-based system offers perspectives for use in a routine clinical practice to deal with abnormal gait (e.g., gait of patients with Parkinson's disease).

5 CONCLUSIONS

We presented a new signal processing algorithm that reduces the number of wearable accelerometers for estimating temporal gait parameters. The advantages of this method can be summarized as follows:

- Only two accelerometers are required, i.e., one for each shoe at the level of the heel. This contributes

to a simplification of our wearable accelerometer-based system, thus resulting in reducing the costs and time needed to attach the system on body.

- This algorithm is validated for consecutive strides during normal walking. The validation used reference data provided by a kinematic system (used as gold standard) and a video camera.
- Compared to previous studies, the proposed method performs equally well or better in terms of accuracy and precision of detection of temporal gait parameters such as times of swing, stance, and stride phases.

The extension of this method to the study of pathological gait (e.g., gait of patients with Parkinson's disease) is now in progress. The method promises to allow an objective quantification of gait parameters in routine clinical practice.

ACKNOWLEDGEMENTS

The authors wish to acknowledge the contribution of J. Stamatakis and B. Macq through the design of the accelerometer-based hardware system used in the present study. The authors would like also to thank all the participants to the gait tests of this study.

REFERENCES

- Aminian, K., Rezakhanlou, K., De Andres, E., Fritsch, C., Leyvraz, P.-F., and Robert, P. (1999). Temporal feature estimation during walking using miniature accelerometers: an analysis of gait improvement after hip arthroplasty. *Medical and Biological Engineering and computing*, 37(6):686–691.
- Auvinet, B., Chaleil, D., and Barrey, E. (1999). Analyse de la marche humaine dans la pratique hospitalière par une méthode accélérométrique. *Revue du Rhumatisme*, 66(7–9):447–457.
- Boutaayamou, M., Schwartz, C., Denoël, V., Forthomme, B., Croisier, J.-L., Garraux, G., Verly, J., and Brûls, O. (2014). Development and validation of a 3D kinematic-based method for determining gait events during overground walking. In *IEEE International Conference on 3D Imaging*, pages 1–6.
- Boutaayamou, M., Schwartz, C., Stamatakis, J., Denoël, V., Maquet, D., Forthomme, B., Croisier, J.-L., Macq, B., Verly, J., Garraux, G., and Brûls, O. (2015a). Development and validation of an accelerometer-based method for quantifying gait events. *Medical Engineering and Physics*, 37:226–232.
- Boutaayamou, M., Denoël, V., Verly, J., Garraux, G., and Brûls, O. (2015b). Gait segmentation using continuous wavelet transform for extracting validated gait events from accelerometer signals. In *Biomedica 2015–The*

- European Life Sciences Summit.*
- Godfrey, A., Conway, R., Meagher, D., and ÓLaighin, G. (2008). Direct measurement of human movement by accelerometry. *Medical Engineering and Physics*, 30(10):1364–1386.
- Forsman, P. M., Toppila, E. M., and Hægström, E. O. (2009). Wavelet analysis to detect gait events. In *IEEE EMBC*, pages 424–427.
- Khandelwal, S., and Wickström, N. (2014). Identification of gait events using expert knowledge and continuous wavelet transform analysis. In *Proceedings of the International Conference on Bio-inspired Systems and Signal Processing*, pages 197–204.
- Lee, J.-A., Cho S.-H., Lee J.-W., Lee K.-H., and Yang H.-K. (2007). Wearable accelerometer system for measuring the temporal parameters of gait. In *Proceedings of the 29th Annual International Conference of the IEEE EMBS*, pages 23–26.
- Rampp, A., Barth, J., Schüle, S., Gaßmann, K.-G., Klucken, J., and Eskofier, B. M. (2015). Inertial sensor-based stride parameter calculation from gait sequences in geriatric patients. *IEEE Transactions on Biomedical Engineering*, 62(4):1089–1097.
- Rueterbories, J., Spaich, E.G., Larsen, B., and Andersen O.K. (2010). Methods for gait event detection and analysis in ambulatory systems. *Medical Engineering and Physics*, 32(6):545–552.
- Salarian, A., Russmann, H., Vingerhoets, F.J.G., Dehollain, C., Blanc, Y., Burkhard P.R., and Aminian, K. (2004). Gait assessment in Parkinson's disease: toward an ambulatory system for long-term monitoring. *IEEE Transactions on Biomedical Engineering*, 51(8):1434–1443.
- Selles, R.W., Formanoy, M.A.G., Bussmann, J.B.J., Janssens, P.J., and Stam, H.J. (2005). Automated estimation of initial and terminal contact timing using accelerometers; development and validation in transtibial amputees and controls. *IEEE Transactions on Neural Systems and Rehabilitation Engineering*, 13(1):81–88.
- Stamatakis, J., Crémers, J., Maquet, D., Macq, B., and Garraux, G. (2011). Gait feature extraction in Parkinson's disease using low-cost accelerometers. In *Proceedings of the Annual International Conference of the IEEE Engineering in Medicine and Biology Society*, pages 7900–7903.
- Whittle, W. (1996). Clinical gait analysis: a review. *Human Movement Science*, 15:369–387.
- Willemsen, A.T.M., Bloemhof, F., and Boom, H.B. (1990). Automatic stance-swing, phase detection from accelerometer data for peroneal nerve stimulation. *IEEE Transactions on Biomedical Engineering*, 37(12):1201–8.

APPENDIX

We present the piecewise-linear fitting method used to estimate the locations of the convex curvature in a

signal (Sec. 2.4.1). For this, we consider a given signal $sig = sig(t_1), sig(t_2), \dots, sig(t_N)$ defined in a time interval $I = t_1, t_2, \dots, t_N$, where N is the total number of samples of sig . This method first computes the coefficients of piecewise-linear functions with two linear segments that best fit sig in the least-square sense, leading to the computation of least-square errors. The minimum of these least-square errors is then determined and the associated piecewise-linear function provides two linear segments that intersect at the breakpoint $(t_b, sig(t_b))$. The main steps to determine the breakpoint $(t_b, sig(t_b))$ are as follows:

- For each $k = 1, \dots, N$, one computes the coefficients $\alpha_1, \alpha_2, \beta_1$, and β_2 of a piecewise-linear function p_k that best fits sig by minimizing

$$E_k = \sum_{i=1}^N (sig(t_i) - p_k(t_i))^2, \quad (2)$$

where

$$p_k(t) = \begin{cases} \alpha_1 * t + \beta_1, & t \in [t_1, t_k], \\ \alpha_2 * t + \beta_2, & t \in]t_k, t_N]. \end{cases} \quad (3)$$

This error can be expressed as

$$E_k = \|A X_k - B\|^2, \quad (4)$$

where

$$X_k = \begin{pmatrix} \alpha_1 \\ \beta_1 \end{pmatrix}, A = \begin{pmatrix} t_1 & 1 \\ \vdots & \vdots \\ t_k & 1 \end{pmatrix},$$

$$B = \begin{pmatrix} sig(t_1) \\ \vdots \\ sig(t_k) \end{pmatrix} \text{ if } t \in [t_1, t_k],$$

and

$$X_k = \begin{pmatrix} \alpha_2 \\ \beta_2 \end{pmatrix}, A = \begin{pmatrix} t_{k+1} & 1 \\ \vdots & \vdots \\ t_N & 1 \end{pmatrix},$$

$$B = \begin{pmatrix} sig(t_{k+1}) \\ \vdots \\ sig(t_N) \end{pmatrix} \text{ if } t \in]t_k, t_N].$$

The normal equations associated with (4) are

$$A^t A X_k = A^t B. \quad (5)$$

Solving (5) leads to the coefficients $\alpha_1, \alpha_2, \beta_1$, and β_2 .

- Finally, one obtains the breakpoint $(t_b, sig(t_b))$ by determining the minimum of the least-square errors, i.e.,

$$E_b = \min_{k=1, \dots, N} (E_k). \quad (6)$$